


# Skeletal stem cell-mediated suppression on inflammatory osteoclastogenesis occurs via concerted action of cell adhesion molecules and osteoprotegerin

Xin Li<sup>1,2,3,4</sup> | Li Ding<sup>1,3</sup> | Yu-Xing Wang<sup>1,5</sup> | Zhong-Li Li<sup>5</sup> | Qian Wang<sup>1,5</sup> | Zhi-Dong Zhao<sup>1,5</sup> | Sen Zhao<sup>1,5</sup> | Hua Wang<sup>1</sup> | Chu-Tse Wu<sup>1</sup> | Ning Mao<sup>2</sup> | Heng Zhu<sup>1,2</sup> 

<sup>1</sup>Beijing Institute of Radiation Medicine, Beijing, People's Republic of China

<sup>2</sup>Beijing Institute of Basic Medical Sciences, Beijing, People's Republic of China

<sup>3</sup>Air Force Medical Center, PLA, Beijing, People's Republic of China

<sup>4</sup>Jizhong Energy Xingtai MIG General Hospital, Xingtai, People's Republic of China

<sup>5</sup>People's Liberation Army General Hospital, Beijing, People's Republic of China

## Correspondence

Heng Zhu, PhD, Beijing Institute of Radiation Medicine, Road Taiping 27, Beijing, 100850, People's Republic of China.  
Email: zhudingdingabc@163.com

Ning Mao, MD, Beijing Institute of Basic Medical Sciences, Road Taiping 27, Beijing, 100850, People's Republic of China.  
Email: maoning3suo@126.com

Li Ding, PhD, Air Force Medical Center, PLA, Road Fucheng 30, Beijing, 100142, People's Republic of China.  
Email: dingli7578@163.com

## Funding information

Beijing Natural Sciences Grants, Grant/Award Numbers: 7192203, 7182123; National Natural Science Foundation of China, Grant/Award Numbers: 81101342, 81371945, 81500083, 81871771, 81572159

## Abstract

In the current study, we investigated how skeletal stem cells (SSCs) modulate inflammatory osteoclast (OC) formation and bone resorption. Notably, we found that intercellular adhesion molecule-1 (ICAM-1), vascular cell adhesion molecule-1 (VCAM-1), and osteoprotegerin (OPG) play a synergistic role in SSC-mediated suppression of inflammatory osteoclastogenesis. The effect of SSCs on inflammatory osteoclastogenesis was investigated using a lipopolysaccharide-induced mouse osteolysis model *in vivo* and human osteoarthritis synovial fluid (OASF) *in vitro*. OC formation was determined by tartrate-resistant acid phosphatase staining. Bone resorption was evaluated by microcomputerized tomography, serum C-terminal telopeptide assay, and pit formation assay. The expression of ICAM-1, VCAM-1, and OPG in SSCs and their contribution to the suppression of osteoclastogenesis were determined by flow cytometry or enzyme linked immunosorbent assay. Gene modification, neutralization antibodies, and tumor necrosis factor- $\alpha$  knockout mice were used to further explore the mechanism. The results demonstrated that SSCs remarkably inhibited inflammatory osteoclastogenesis *in vivo* and *in vitro*. Mechanistically, inflammatory OASF stimulated ICAM-1 and VCAM-1 expression as well as OPG secretion by SSCs. In addition, ICAM-1 and VCAM-1 recruited CD11b<sup>+</sup> OC progenitors to proximity with SSCs, which strengthened the inhibitory effects of SSC-derived OPG on osteoclastogenesis. Furthermore, it was revealed that tumor necrosis factor  $\alpha$  is closely involved in the suppressive effects. In summary, SSCs express a higher level of ICAM-1 and VCAM-1 and produce more OPG in inflammatory microenvironments, which are sufficient to inhibit osteoclastogenesis in a "capture and educate" manner. These results may represent a synergistic mechanism to prevent bone erosion during joint inflammation by SSCs.

## KEYWORDS

cell adhesion molecules, inflammatory osteoclastogenesis, osteoprotegerin, skeletal stem cells

Xin Li, Li Ding, and Yu-Xing Wang contributed equally to this study.

This is an open access article under the terms of the Creative Commons Attribution-NonCommercial-NoDerivs License, which permits use and distribution in any medium, provided the original work is properly cited, the use is non-commercial and no modifications or adaptations are made.

© 2019 The Authors. STEM CELLS TRANSLATIONAL MEDICINE published by Wiley Periodicals, Inc. on behalf of AlphaMed Press

## 1 | INTRODUCTION

Skeletal stem cells (SSCs) have been defined as tissue-specific stem cells in skeletons and have been demonstrated to play pivotal roles in maintaining and repairing skeletal tissues.<sup>1-8</sup> By determining unique cell surface marker profiles and performing rigorous functional characterizations, previous researchers have identified a number of subpopulations of stem and progenitor cells from skeletal tissues, including bone, cartilage, and tendon.<sup>1-8</sup> Chan et al showed the presence of CD45-Ter119-Tie2-AlphaV+ multipotent stem cells in murine bone and identified cells and factors in the SSC niches that regulate its activity.<sup>2</sup> Another study demonstrated that Gremlin-1 defines a population of osteochondral reticular stem cells in murine bone marrow. Functional assays determined that these cells are needed for bone development, bone remodeling, and fracture repair.<sup>3</sup> Moreover, the recent identification of self-renewing and multipotent SSCs in human bones further validated the presence of endogenous stem cells in skeletal tissue.<sup>8</sup> However, most studies described in these reports focus on SSC differentiation into osteoblastic lineage cells and their contribution to bone formation. Most importantly, the effect of SSCs on bone-resorbing cells, which eat and remodel bones, was overlooked.

Osteoclasts (OCs) are the most potent bone-resorbing cells.<sup>9-11</sup> By encoding tartrate-resistant acid phosphatase (TRAP) and secreting acid and lytic enzymes, mature, multinucleated OCs produce pits in bone or elephant tusk slices *in vitro* and degrade bone *in vivo*. They also promote the release of bone-resorbing substrates, such as serum C-terminal telopeptide (CTX). The process is also accompanied by the expression of osteoclastic genes, including nuclear factor of activated T cells 1 (NF-ATc1), c-Fos, c-Fms, receptor activator of NF- $\kappa$ B (RANK), dendrocyte expressed seven transmembrane protein (DC-STAMP), and cathepsin K. Notably, accumulating studies indicate that OCs are involved in the initiation and progression of inflammatory bone diseases, including osteoarthritis.<sup>9-11</sup> The increase of proinflammatory cytokines, such as interleukin-1  $\beta$  (IL-1 $\beta$ ), tumor necrosis factor- $\alpha$  (TNF- $\alpha$ ), and interleukin-17A (IL-17A), in osteoarthritis synovial fluid (OASF) or subchondral bones lead to overactive OC formation and joint damage.<sup>12-14</sup> Moreover, cell surface molecules in bone stromal cells typically act as pro-osteoclastic factors.<sup>15-18</sup> Furthermore, inflammatory osteoclastogenesis was reported to contribute to bone infection-induced osteoporosis. Bacteria-derived molecules, such as lipopolysaccharide (LPS), promote the release of pro-osteoclastic factors and cause systemic bone lesion.

Thus, we suggest that OCs may be a pivotal cell target for the alleviation of inflammatory skeletal lesions, such as osteoarthritis and bone infection. Osteoprotegerin (OPG), a soluble decoy receptor of the receptor activator of NF- $\kappa$ B ligand (RANKL), which is typically produced by connective tissue cells, has been identified as the most potent inhibitor of OC formation.<sup>19-21</sup> However, this cell-derived OPG typically works in a paracrine manner, which may limit its anti-osteoclastic effects. Therefore, it is interesting to investigate how OPG controls osteoclastogenesis in skeletal tissues.

We have pursued the identification of SSCs and the exploration of SSC-mediated regulation over the past decade.<sup>22-24</sup> Our previous studies revealed the pivotal role of SSCs in controlling the inflammatory

### Significance statement

Skeletal stem cells (SSCs), tissue-specific stem cells from the skeleton, have been highlighted in recent scientific research and translational medicine. Although SSCs have been shown to contribute to skeletal development and regeneration, the regulation in osteoclastogenesis, the bone remodeling, and the application potential of SSCs in inflammatory bone diseases are incompletely understood. This study indicates a population of murine long-bone-derived SSCs have the potential to induce the expression of OPG, as well as ICAM-1 and VCAM-1 under inflammatory microenvironments and suppressed inflammatory osteoclast formation and bone resorption *in vivo* and *in vitro*. These findings indicate the possibility of using SSCs to alleviate bone loss in diseases.

response. We showed that intravenous infusion of murine SSCs could alter the phenotype and function of splenic lymphocytes, which ameliorate the inflammatory tissue damage.<sup>25</sup> Further investigation demonstrated that murine SSCs alter the migratory property of T and dendritic cells and delay the development of murine lethal acute graft-versus-host disease.<sup>26</sup> Our recent study showed that SSCs are capable of attenuating poly (lactic-co-glycolic) acid-induced inflammatory responses by inhibiting host dendritic cell maturation and function.<sup>27</sup>

Given the fundamental role of OCs in inflammatory bone lesions and the potent immunoregulatory properties of SSCs, an effective strategy for alleviating inflammatory bone diseases may be via targeting OCs. In the present study, we explored the effects of SSCs on inflammatory osteoclastogenesis and the subsequent bone resorption. Moreover, the cellular and molecular mechanisms underlying the capacity of SSCs to regulate inflammatory osteoclastogenesis were also investigated.

## 2 | MATERIALS AND METHODS

### 2.1 | Animals

Normal inbred 2-week-old C57BL/6 mice ( $n = 20$ ) and 8-week-old BALB/c mice ( $n = 300$ ) were purchased from the Laboratory Animal Center of the Academy of Military Medical Sciences of China (Beijing). The tumor necrosis factor  $\alpha$  knockout mice (TNF- $\alpha$  KO mice) were obtained from the Jackson Laboratory. All the experiments were performed in accordance with the Academy of Military Medical Sciences Guide for Laboratory Animals.

### 2.2 | Osteoarthritis patients and samples

The synovial fluid from osteoarthritis patients (OASF) is a potent inflammatory mediator, which includes numerous inflammatory

cytokines and has been reported to promote osteo-chondral lesion in osteoarthritis. In the current study, OASF was used to mimic the joint microenvironments of osteoarthritis and investigate the potential role of SSCs in inflammatory osteoclastogenesis. Briefly, human OASF was aspirated from the knee joints of 10 patients with osteoarthritis (OA) (3 males and 7 females, average age 60.7 years, average BMI 25.3 kg/m, average disease duration 6.8 years) (Table S1). The OASF was further purified by centrifugation at 3000 revolutions per minute for 15 minutes, and the supernatants were harvested for further investigation. All patients met the American College of Rheumatology criteria for the classification of knee OA.<sup>28,29</sup> They were classified as Kellgren-Lawrence grade 3 or 4, with synovial cavity effusion of grade 2 or 3 according to their whole-organ magnetic resonance imaging score (WOMRS), (grade 0, normal; grade 1, less than 33% of maximum potential distension; grade 2, 33% to 66% of maximum potential distension; and grade 3, greater than 66% of maximum potential distension).<sup>28,29</sup> The exclusion criteria included a history of inflammatory arthritis, previous knee surgery or knee injection, or metastatic cancer. Ethics approval was obtained from the hospital Research Ethics Committee, and participant consent was acquired prior to the collection of samples.

### 2.3 | SSC preparation

In the current study, murine SSCs were cultured from mouse long bones according to a method we previously established with minor revision.<sup>23</sup> Briefly, femurs and tibiae from 2-week-old C57BL/6 mice ( $n = 20$ ) were dissected, and the bone marrow cells were flushed out. The whole long bones were chopped and then digested by collagenase II (Sigma, 3050 Spruce Street, Saint Louis, MO 63103, USA, 0.1% vol/vol) at 37°C for 1 hour. The bone chips were cultured in minimum essential medium eagle, alpha modification ( $\alpha$ -MEM; Invitrogen, Carlsbad, California) supplemented with 10% fetal bovine serum (FBS; Hyclone, Logan, Utah). The adherent cells at passages 3-6 were used for in vivo and in vitro experiments unless otherwise described.

To investigate the underlying mechanisms of SSCs in inflammatory osteoclastogenesis, the expression of OPG was genetically knocked down in SSC-like cells (C3H10T1/2, ATCC) by using commercial lentiviral products (Shanghai Genechem Co., Ltd). The ICAM-1<sup>high</sup> SSCs (C3H10T1/2-ICAM-1 overexpression) and VCAM-1<sup>high</sup> SSCs (C3H10T1/2-VCAM-1 overexpression) previously prepared and maintained in our lab were also used in the current study.<sup>30,31</sup>

### 2.4 | SSC infusion of a mouse inflammatory bone resorption model

LPS infusion into mice typically causes inflammatory responses and overactive osteoclastogenesis.<sup>32-34</sup> To investigate the effects of SSCs on inflammatory osteoclastogenesis in vivo, SSCs were administered to mice via the tail vein. Briefly, LPS was administered to 8-week-old Balb/c mice via a single intraperitoneal injection of 200  $\mu$ g in 100  $\mu$ L PBS per mouse (LPS mice). Shortly afterwards, graded doses of SSC ( $0, 1 \times 10^5$

and  $5 \times 10^5$  SSC per mouse) were administered to the mice via tail vein injection. For mechanistic investigation, ICAM-1<sup>high</sup> SSCs, VCAM-1<sup>high</sup> SSCs, and OPG knocked-down SSCs (OPG<sup>low</sup> SSCs) were intravenously administered to the LPS mice ( $5 \times 10^5$  SSC per mouse,  $n = 6$ ), respectively. The control group mice received PBS (PBS mice) instead of SSCs.

For the in situ osteoclastogenesis assay, eight mice per group were sacrificed at day 7 post SSC injection, and the murine tibiae were harvested ( $n = 8$ ). The specimens were fixed in 10% neutral buffered formalin, imbedded in paraffin, demineralized in edetic acid disodium salt decalcified solution, and cut into 5- $\mu$ m-thick sections. OC formation was determined by TRAP staining. For the CTX assay, the sera were obtained from six mice per group 21 days after SSC injection ( $n = 4$ ). All plasma samples were freshly isolated by centrifugation. To detect the mRNA expression of osteoclastic genes in mice, six mice per group were sacrificed 5 days post SSC infusion ( $n = 4$ ), and bone marrow cells were harvested by centrifugation for further determination via real-time quantitative polymerase chain reaction (RT-qPCR).

### 2.5 | Micro computerized tomography ( $\mu$ CT) analysis

Murine femurs were harvested 21 days after SSC injection ( $n = 4$ ). The femurs were then fixed overnight in 10% neutral buffered formalin, washed twice in PBS, and stored in 70% ethanol at 4°C for further analysis.  $\mu$ CT scanning and analysis were performed by using a Scanco  $\mu$ CT-40 (Scanco Medical). The bones were scanned at a resolution of 8  $\mu$ m, and reconstruction of three-dimensional (3D) images was performed using a standard convolution back-projection. The bone volume/tissue volume ratio (BV/TV) was calculated by measuring 3D distances directly in the trabecular network.

### 2.6 | TRAP staining

TRAP is a specific marker for osteoclast formation.<sup>33</sup> TRAP staining was performed using a commercial TRAP staining kit (Sigma-Aldrich, St. Louis, Missouri) according to the manufacturer's protocol. For section slice staining, the TRAP staining solution was directly added and incubated for 1 hour. The slices were then washed with PBS and observed under a light microscope (Nikon TE2000-U). To determine OC formation in cell culture plates, the culture medium was discarded, and the cell layers were fixed in citrate-buffered 60% acetone solution (pH 5.4) for at least 30 seconds, washed twice with distilled water, and air-dried. TRAP-positive (TRAP+) multinucleated cells (3 or more nuclei, TRAP+ MNCs) were manually counted under a light microscope (Nikon TE2000-U).

### 2.7 | SSC-involved osteoclast generation in the presence of human OASF

Murine monocytes were purified from the bone marrow mononuclear cells of 8-week-old BALB/c mice using the magnetic-activated cell

sorting (MACS) CD11b<sup>+</sup> Isolation Kit (Miltenyi Biotec, Bergisch Gladbach, Germany). To generate osteoclasts, murine monocytes were cultured in 48-well-plates ( $2 \times 10^3$  monocytes per well) with the addition of human OASF (20% vol/vol). To investigate the effect of SSCs on osteoclastogenesis, SSCs ( $2 \times 10^3$  SSC per well) were added into the *in vitro* OC culture system. To further validate the suppressive effect of SSCs, pro-osteoclastic cytokines, murine macrophage colony-stimulating factor (M-CSF, 20 ng/mL) and murine RANKL (20 ng/mL) were added to the previously described *in vitro* culture system. OC formation was determined by TRAP staining at day 5 after initial culture, and the osteoclasts were counted under a light microscope ( $n = 6$ ).

To exclude the possibility that osteoclastic genes decrease due to a relatively decreased number of OCs among the mixed cell population for gene analysis, the OCs were generated by advantage of a 0.4- $\mu$ m-pore-size membrane Transwell system (Coring) as previously employed by our group. Briefly, SSCs were cultured on the reverse side of the chamber membrane, while CD11b<sup>+</sup> OC precursors were seeded on the upper side of the chamber membrane. After coculture for 5 days, the OCs were harvested from the upper chamber without SSC contamination ( $n = 4$ ). The osteoclastic genes in the cocultured SSCs/OCs or OCs generated in the Transwell system were assayed, respectively.

To mechanistically investigate the suppressive effects of SSCs on OAS-induced osteoclast formation, neutralization antibodies, including anti-TNF- $\alpha$ , anti-IFN- $\gamma$ , anti-IL-17A, anti-M-CSF, and anti-IL-6, were added to the SSC/OASF culture system (200 ng/mL). The TRAP + osteoclasts were counted ( $n = 6$ ).

## 2.8 | Bone resorption pit formation assay

The bone-resorbing activity of OCs was assessed using sterile elephant tusk slices prepared from discarded elephant tusks (Osteosite Dentine Discs, IDS Ltd). The tusk slices (5 mm diameter and 0.3 mm thickness,  $n = 6$ ) were washed three times with culture medium before they were carefully placed at the bottom of the wells of a 48-well cell culture plate. SSCs were seeded onto each slice at a density of  $1 \times 10^4$  per well. The murine CD11b<sup>+</sup> monocytes were added after 24 hours at a density of  $1 \times 10^4$  per well. The OC culture medium (20 ng/mL M-CSF and 20 ng/mL RANKL) supplemented with 10% (vol/vol) OASF was changed every 2 days. The culture was maintained for 3 weeks. The cells on the tusk slices were removed via ultrasonic treatment. The cell-free tusk slices were stained with Toluidine blue to detect resorption pits under a light microscope. The percentage of resorption pits was estimated using the computerized image analysis software Image-Pro Plus (IPP) 6.0. The cell culture medium was harvested from the dentine slice-based resorption system for CTX assay ( $n = 6$ ).

## 2.9 | CTX assay

CTXs are bone collagen degradation products released into the circulation during bone resorption, and an enhancement of osteoclastic

activity causes the accumulation of CTXs *in vivo*.<sup>33</sup> Thus, bone resorptions were further evaluated by measuring the serum levels of CTX in mice. In the current study, the CTX levels in the murine serum and cell culture supernatant were determined by using a commercial kit on serum samples according to the manufacturer's instructions (Nordic Bioscience Diagnostics). All plasma samples and cell culture supernatant were freshly isolated by centrifugation and filtered to deplete cellular components.

## 2.10 | Effect of OASF on cell surface molecules and OPG by SSCs

The expression of intercellular adhesion molecule-1 (ICAM-1) and vascular cell adhesion molecule-1 (VCAM-1) of SSCs was analyzed with flow cytometry. Briefly, the SSCs were seeded into a six-well-plate at a density of  $5 \times 10^5$  per well and were treated with OASF (20%, vol/vol) for 72 hours. The SSCs in each group were stained with FITC- or PE-conjugated monoclonal antibodies against mouse ICAM-1 and VCAM-1 (eBio-Science, San Diego), respectively. The SSC were assayed with a FACSCalibur instrument (Becton Dickinson, San Jose, California), and the data were analyzed using WinMdi 2.8 software.

The OPG expression of SSCs was evaluated by ELISA assay. In brief, SSCs were seeded in 24-well plates at a density of  $2 \times 10^5$  per well and starved in serum-free  $\alpha$ -MEM for a minimum of 6 hours before stimulation with human OASF (20%, vol/vol,  $n = 6$ ) for 8 hours. The culture media were changed to serum-free  $\alpha$ -MEM for an additional 8 hours. The culture supernatants were harvested and filtered to deplete cellular components. The concentrations of mouse OPG in the supernatants were determined according to the manufacturer's protocol of the quantitative determination kit of mouse OPG (R&D Systems, Minneapolis, Minnesota: MOP00). The optical density was read at 450 nm. For each experimental culture well, duplicate ELISA readings were obtained.

To investigate the mechanisms by which OASF-induced expression of adhesion molecules and OPG, numerous neutralization antibodies (anti-TNF- $\alpha$ , anti-IFN- $\gamma$ , anti-IL-17A, anti-M-CSF, and anti-IL-6) were added into the SSC/OC culture system (200 ng/mL). The OPG in the culture medium of each group were detected by ELISA assay. The ratios of ICAM-1- or VCAM-1-expressing SSCs in each group were determined by flow cytometry.

## 2.11 | SSC/OC progenitor adhesion assay

The SSC/OC progenitor adhesion assay was performed according to a published protocol with minor revision.<sup>35</sup> Briefly, SSCs were seeded into a six-well-plate at a density of  $5 \times 10^5$  per well and were pretreated with OASF (20%, vol/vol) for 24 hours. The murine bone marrow mononuclear cells were harvested from mouse (6-8 weeks old) femur and tibia bone marrow suspensions with Ficoll-Paque (1.073 g/mL; Invitrogen) density gradient centrifugation. Furthermore, bone marrow mononuclear cells were suspended at a concentration

of  $10^7$  cells/mL in PBS that contained 2% FBS (Hyclone) and stained with  $10 \mu\text{M}$  carboxyfluorescein diacetate succinimidyl ester (CFSE). After 20 minutes of incubation, the CFSE incorporation was blocked with a large excess of PBS that contained 2% FBS. The CFSE-labeled cells were cocultured with the OASF pretreated SSC for 2 hours. The ratio of SSCs to bone marrow cells was 1:10. The plates were rotated at 300 revolutions per minute for 15 minutes. After washing with cold PBS three times to remove the nonattached bone marrow cells, all cells were trypsinized and labeled by phycoerythrin (PE)-conjugated monoclonal antibodies against murine CD11b. Osteoclast precursor cells were identified by CFSE fluorescence and CD11b expression. Antimouse ICAM-1 or antimouse VCAM-1 blocking antibodies were added (20 and 100 ng/mL) to some treatments.

## 2.12 | RNA interference and neutralization of SSC-derived OPG

To investigate the role of secretory factors in SSC-mediated osteoclastogenesis inhibition, SSCs ( $2 \times 10^3$  SSC per well) were cultured in the lower compartment of Transwell chambers with a  $0.4\text{-}\mu\text{m}$ -pore-size membrane with CD11b<sup>+</sup> monocytes ( $2 \times 10^3$  CD11b<sup>+</sup> per well) in the upper compartment. The TRAP<sup>+</sup> MNCs were counted 7 days after initial culture ( $n = 6$ ). In addition, the expression of OPG in SSCs was blocked by RNA interference and antineutralization antibody. For the RNAi assay, the murine OPG targeting siRNAs for OPG and a negative control (NC) were obtained from Ribobio (www.ribobio.com). The RNA interference

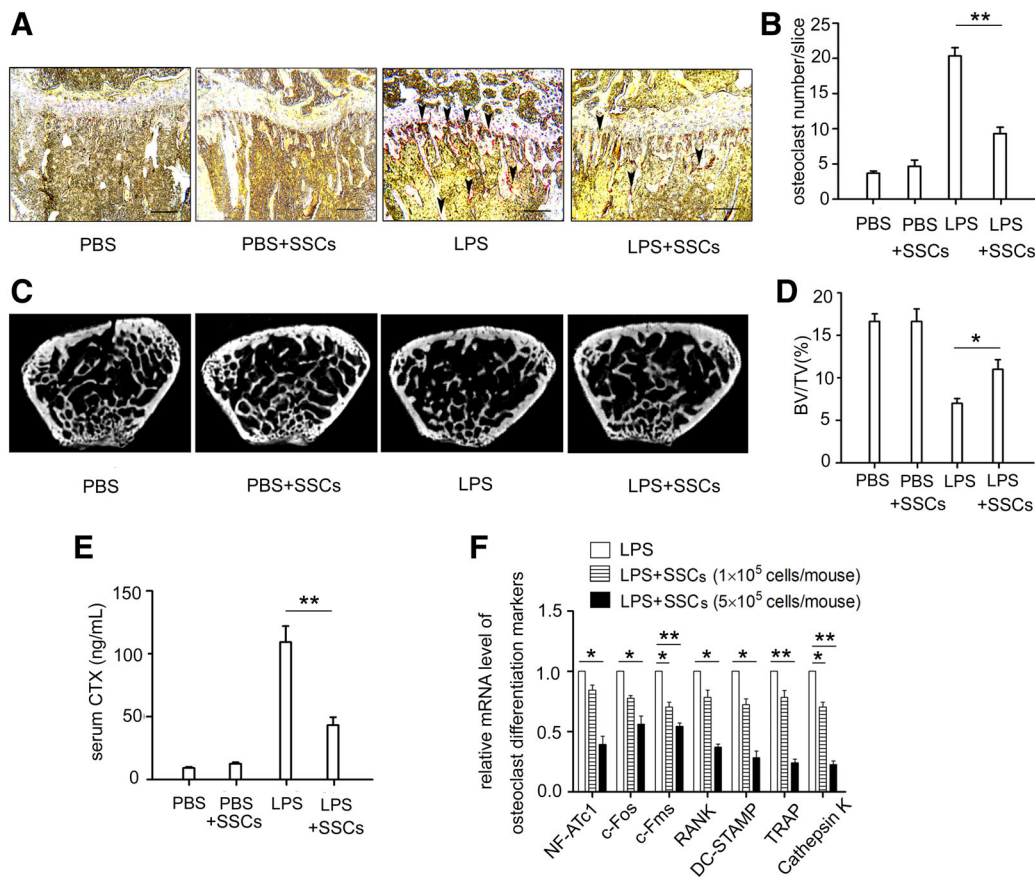


**FIGURE 1** Skeletal stem cells (SSCs) suppressed inflammatory osteoclastogenesis and bone resorption in a lipopolysaccharide (LPS)-induced murine model. A, The osteoclasts were determined by tartrate-resistant acid phosphatase (TRAP) staining. Arrowheads indicate TRAP<sup>+</sup> osteoclasts stained in red in murine tibial metaphysis. Intravenously administered PBS (100  $\mu\text{L}$  PBS per mouse) or SSCs ( $0, 1 \times 10^5, 5 \times 10^5$  SSCs in 100  $\mu\text{L}$  PBS per mouse) did not significantly affect the osteoclast formation in murine bone trabecula. Intraperitoneal LPS injection (200  $\mu\text{g}$  LPS in 100  $\mu\text{L}$  PBS per mouse) caused a remarkable increase in the number of in situ osteoclasts in mice, whereas SSC injections ( $1 \times 10^5, 5 \times 10^5$  SSC in 100  $\mu\text{L}$  PBS per mouse) at the same time significantly inhibited the LPS-induced osteoclastogenesis. Bars represent 500  $\mu\text{m}$ . B,  $^{**}P < .01$  compared with LPS injected mice,  $n = 8$ . C, In addition, the BV/TV (by  $\mu\text{CT}$  analysis) was examined 3 weeks after SSC infusion. Infused SSC partly rescued the decrease in the BV/TV induced by LPS injection. D,  $^{*}P < .05$  compared with LPS injected mice,  $n = 4$ . E, Furthermore, serum C-terminal telopeptide (CTX) was assayed 3 weeks post SSC administration. SSC significantly decreased the serum level of CTX in LPS mice.  $^{*}P < .05$  compared with LPS injected mice,  $n = 4$ . F, Moreover, the mRNA expression of osteoclastic genes in murine bone marrow cells was determined (by quantitative PCR) 5 days after SSC infusion. SSC remarkably suppressed the expression of osteoclastic markers in the bone marrow of LPS mice in an SSC dose-dependent manner.  $^{*}P < .05$ ;  $^{**}P < .01$ , compared with LPS injected mice,  $n = 4$

(RNAi) experiments were performed according to the manufacturer's protocol. SSC were seeded on six-well plates at a density of  $5 \times 10^5$  cells/well; when the cells reached 60%-80% confluence, mimic (10 nM) and NC (10 nM) siRNAs were each mixed with RNA transfection buffer (ribo FECT CP) before being added to the SSCs culture medium. The OPG-RNAi-SSC were used for the SSC/OC culture as previously described ( $n = 6$ ). For the antibody neutralization assay, the antimouse OPG-neutralization antibody (200 ng/mL) was directly added to the SSC/OC coculture according to the manufacturer' protocols ( $n = 6$ ). The TRAP+ MNCs in the RNAi experiments and antibody neutralization experiments were counted 7 days after initial culture.

## 2.13 | Generation of TNF- $\alpha$ deficient inflammatory serum using TNF- $\alpha$ -KO mice

To further investigate the role of TNF- $\alpha$  in SSC-mediated suppression of inflammatory osteoclastogenesis, LPS were intraperitoneally administered to 8-week-old TNF- $\alpha$  KO mice and their wild-type counterparts by a single injection of 200  $\mu$ g in 100  $\mu$ L PBS per mouse. After 3 days, the mice were sacrificed, and the serum was generated from peripheral blood by centrifugation at 3000 revolutions per minute for 15 minutes. The serum was filtered using a 0.4- $\mu$ m-pore-size membrane to remove the possible cellular contamination before addition to the SSC/OC coculture system (20%, vol/vol).

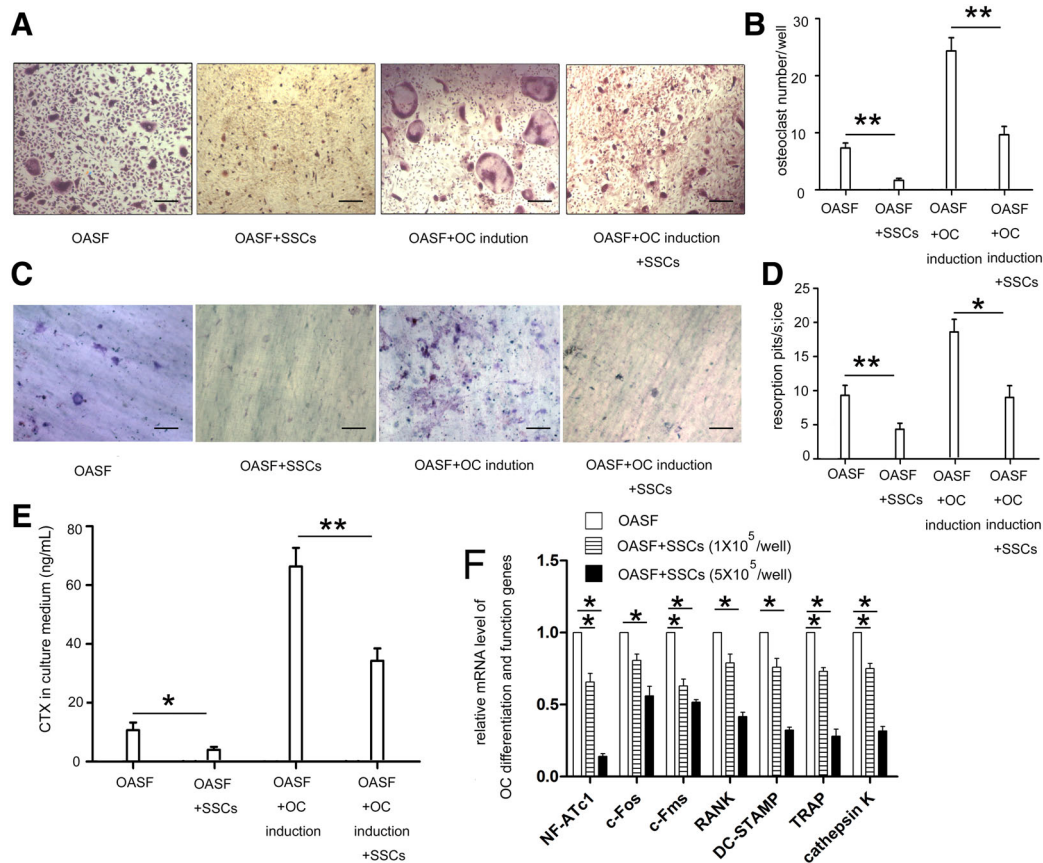


**FIGURE 2** Skeletal stem cells (SSCs) inhibited osteoclastic differentiation and pit formation in the presence of human osteoarthritis synovial fluids (OASF). A, Murine CD11b<sup>+</sup> bone marrow monocytes were cultured in 48-well-plates ( $2 \times 10^3$  monocytes per well) in the presence of human OASF (20% vol/vol). The osteoclasts in culture plates were determined by tartrate-resistant acid phosphatase (TRAP) staining after 7 days. TRAP+ multinucleated cells (3 or more nuclei) were manually counted under a light microscope. In some groups, SSCs ( $2 \times 10^3$  SSCs per well) were added in the previously described in vitro OC culture system. The results of TRAP staining showed that SSCs inhibited OASF-induced osteoclastogenesis. To further validate the suppressive effect of SSCs, pro-osteoclastic cytokines murine M-CSF (20 ng/mL) and murine RANKL (20 ng/mL) were added into the previously described in vitro culture system, which yielded more osteoclasts in plate wells as expected. Notably, SSCs ( $2 \times 10^3$  SSCs per well) exhibited strong suppressive effects on osteoclastogenesis that were induced by both OASF and pro-osteoclastic cytokines. Bars represent 200  $\mu$ m. B,  $**P < .01$  compared with no-SSC control,  $n = 6$ . C, In addition, the pit formation assays were performed on the dentine slices (diameter 5 mm, thickness 0.3 mm) by culturing osteoclasts in four groups as previously described for 3 weeks. The pits were determined by Toluidine blue staining. D, The percentage of resorption pits was estimated using computerized image analysis software. SSCs significantly suppressed pit formation induced by inflammatory osteoclastogenesis in vitro.  $*P < .05$ ;  $**P < .01$  compared with no-SSC control,  $n = 6$ . E, Furthermore, the CTX in culture medium was detected after 3 weeks to validate the suppressive effects of SSCs on inflammatory resorptions.  $*P < .05$ ;  $**P < .01$  compared with the no-SSC control,  $n = 6$ . F, Moreover, the osteoclastic genes in the SSC/osteoclast system (0,  $1 \times 10^5$ ,  $5 \times 10^5$  SSC, and  $1 \times 10^5$  CD11b<sup>+</sup> monocytes per well of six-well plates) were determined at day 5. SSC significantly suppressed the expression of osteoclastic markers in the presence of human OASF in an SSC dose-dependent manner.  $*P < .05$ , compared with human OASF group,  $n = 6$

## 2.14 | Statistical analysis

Data are represented as the mean values with standard deviations. Statistical significance was analysed using Student's t test and one way ANOVA. P values less than 0.05 were considered to be significant.

## 3 | RESULTS

### 3.1 | Intravenous infusion of SSCs suppressed murine inflammatory osteoclastogenesis and bone resorption

Approximately  $5 \times 10^7$  cells (passage 4) were harvested in each mouse before the experiments. As shown in Figure 1A,B, intravenously administered SSCs did not significantly affect OC formation in

the PBS mice. However, the results of TRAP+ staining on bone slices demonstrated that infused SSCs caused a decrease in the number of in situ osteoclasts by >50% in the LPS mice (\*\* $P < .01$ ).

To examine the influence of SSCs on the resorbing function of OCs,  $\mu$ CT analysis of trabecular bone in the distal epiphyses of femurs was performed 3 weeks post LPS and/or post SSC injections. Interestingly, the decrease in the BV/TV induced by LPS was partly rescued by the SSC infusion (Figure 1C,D) (\* $P < .05$ ). Consistent with the  $\mu$ CT data, LPS caused a remarkable increase in the CTX levels, while SSCs significantly decreased the serum level of CTX in the mice (Figure 1E) (\*\* $P < .01$ ).

We further tested the in vivo effects of SSCs on the expression of OC differentiation markers. Notably, the expressions of NF-ATc1, c-Fos, c-Fms, RANK, DC-STAMP, TRAP, and cathepsin K in bone marrow cells were significantly increased in the LPS mice. Promisingly, SSCs remarkably reduced the expression of osteoclastic markers in the bone marrow of the LPS mice (Figure 1F). Moreover, the

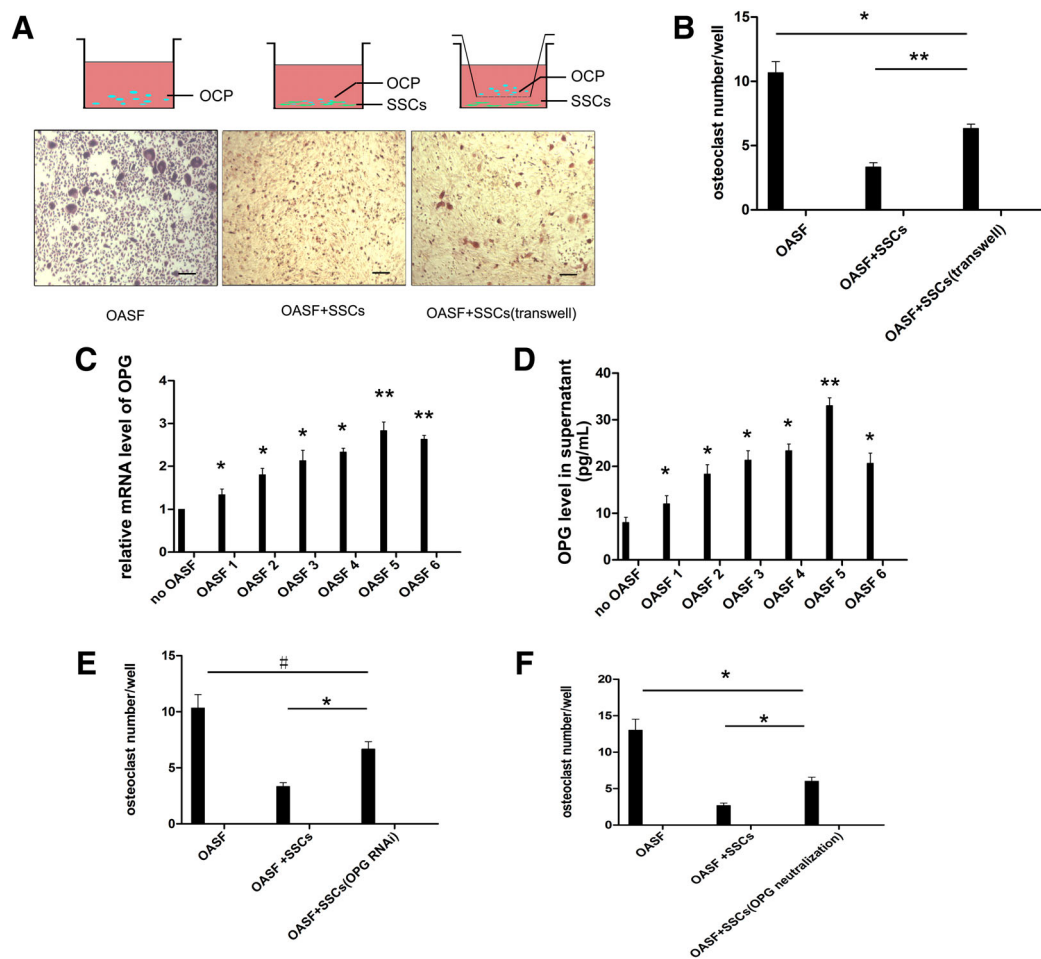


**FIGURE 3** Skeletal stem cells (SSCs) suppress inflammatory osteoclast (OC) formation through secreted osteoprotegerin (OPG). SSCs ( $2 \times 10^3$  SSCs per well) were cultured in the lower compartment of Transwell chambers with a  $0.4\text{-}\mu\text{m}$ -pore-size membrane, with  $\text{CD11b}^+$  monocytes ( $2 \times 10^3$   $\text{CD11b}^+$  per well) in the upper compartment. SSC maintained the inhibitory effects without cell-cell contact. Bars represent  $200\ \mu\text{m}$ . B, The tartrate-resistant acid phosphatase positive (TRAP+) osteoclast formation partially recovered. \*\* $P < .01$ , compared with no-Transwell group,  $n = 5$ . In addition, (C) OPG mRNA expression in SSCs and (D) SSC-secreted OPG were detected by quantitative PCR and ELISA, respectively. Both mRNA expression and protein secretion by SSCs were remarkably elevated in the presence of human osteoarthritis synovial fluid (OASF). \* $P < .05$ ; \*\* $P < .01$ , compared with no-OASF group,  $n = 6$ . E, Furthermore, the TRAP+ osteoclast formation in the SSC/OC coculture system ( $2 \times 10^3$  SSC and  $2 \times 10^3$   $\text{CD11b}^+$  monocytes per well) was partially rescued when OPG in SSC were blocked with OPG-targeted RNAi and (F) an anti-OPG-neutralization antibody ( $200\ \text{ng/mL}$ ). \* $P < .05$ , compared with NC groups,  $n = 6$

suppressive effect was SSC dose-dependent (Figure 1F) ( $*P < .05$ ;  $**P < .01$ ). Therefore, these results suggest that SSC infusion significantly suppresses OC formation and bone resorption in proinflammatory microenvironments *in vivo*, but it does not affect the osteoclastic activity in noninflammatory mice.

### 3.2 | SSCs inhibited OC differentiation and pit formation in the presence of human OASF

SSCs and CD11b<sup>+</sup> monocytes were cocultured in the presence of OASF (10%, vol/vol) with/without M-CSF (20 ng/mL) and RANKL (20 ng/mL) to investigate the influence of OASF on SSC-mediated osteoclastogenesis. After culturing for 9 days, the cells were stained, and the TRAP<sup>+</sup> multinucleated cells were counted. The results of the SSC-involved OC generation experiments showed that SSCs inhibit OC formation in the presence of human OASF (Figure 2A,B) ( $**P < .01$ ). In addition, they inhibited OC formation in osteoclastic induction medium (Figure 2A,B) ( $**P < .01$ ). Further investigation demonstrated that the SSCs also suppressed the resorbing function of OCs in the presence of human OASF. The results of the pit formation analysis showed that OCs produced fewer resorption pits on dentine slices in the presence of SSCs (Figure 2C,D) ( $*P < .05$ ;  $**P < .01$ ). Moreover, SSCs significantly decreased the serum level of CTX in the pit formation assay (Figure 2E) ( $*P < .05$ ;  $**P < .01$ ). The results of

Q-PCR showed that SSCs suppressed the expression of osteoclastic genes, including NF-ATc1, c-Fos, c-Fms, RANK, DC-STAMP, TRAP, and cathepsin K, in an SSC dose-dependent manner (Figure 2F) ( $*P < .05$ ). The OCs generated in the Transwell system exhibited a similar osteoclastic gene expression profile (Figure S2). In conclusion, these data suggest that SSCs are capable of inhibiting osteoclastic activity in the OA joint microenvironment.

### 3.3 | SSCs suppress inflammatory OC formation through secreted OPG acting in synergy with ICAM-1 and VCAM-1

To better understand the underlying mechanisms of the suppressive effects, a Transwell assay was performed. Although SSCs maintained their inhibitory effects without cellular contact, OC formation partially recovered (Figure 3A,) ( $**P < .01$ ). These data strongly suggested that both soluble factors and cell surface molecules were involved in the SSC-mediated osteoclastic suppression. Since OPG is a central inhibitory factor of osteoclastogenesis,<sup>19-21</sup> we then examined whether there were changes in the OPG expression in SSCs in response to human OASF. The RT-qPCR and ELISA results showed a significant elevation in the OPG mRNA expression and protein secretion by SSCs after OASF incubation (Figure 3C,D) ( $*P < .05$ ;  $**P < .01$ ). We further blocked OPG expression in SSCs with OPG-targeted RNAi (Figure 3E)

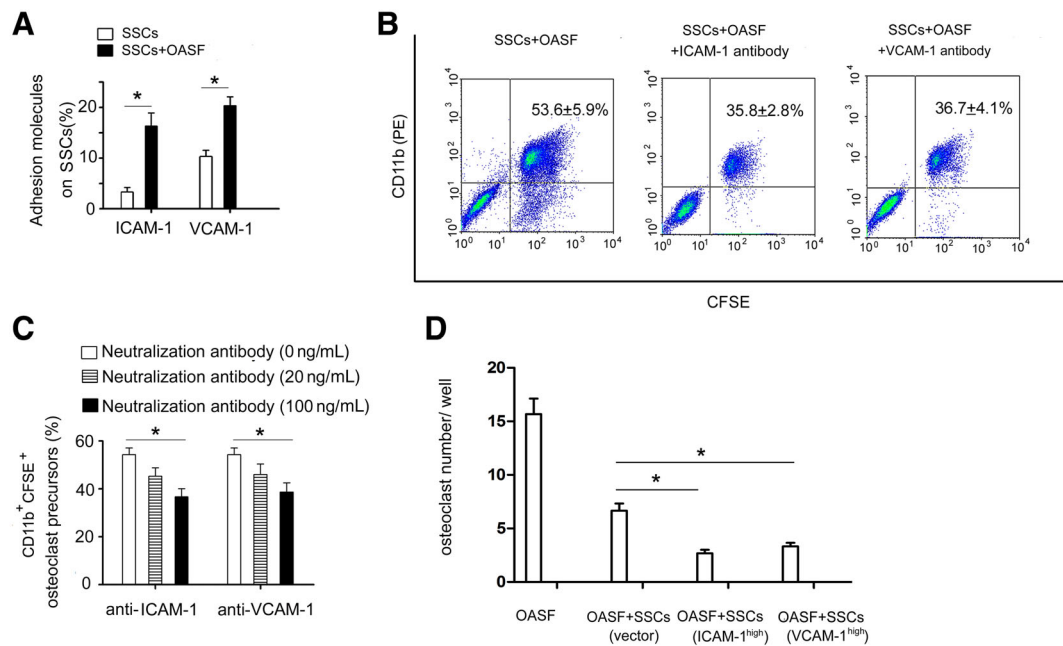


**FIGURE 4** High expression of ICAM-1 and VCAM-1 contribute to capturing osteoclast (OC) progenitors by skeletal stem cells (SSCs). A, The expressions of ICAM-1 and VCAM-1 on the surface were detected by flow cytometry. Incubation with human osteoarthritis synovial fluid (OASF) (20% vol/vol) for 3 days caused significant increases of ICAM-1<sup>+</sup> SSC and VCAM-1<sup>+</sup> SSCs in the total SSC population.  $*P < .05$ , compared with no human OASF groups,  $n = 6$ . B, The fluorescent dye (CFSE)-labeled bone marrow cells were cocultured with OASF-pretreated SSC to enable SSC capturing CD11b<sup>+</sup> progenitors. The CFSE-labeled CD11b<sup>+</sup> osteoclast progenitors were determined flow cytometry. Blockage of ICAM-1 and VCAM-1 using neutralization antibodies (0, 20, and 100 ng/mL) inhibited SSCs in capturing CD11b<sup>+</sup> cells. C, The suppressive effect occurs in an antibody dose-dependent manner.  $*P < .05$ , compared with no-neutralization antibody groups,  $n = 6$ . D, Moreover, the addition of neutralization antibodies against ICAM-1 and VCAM-1 leads to a decrease in OC number in the SSC/OC cocultured system.  $*P < .05$ , compared with empty vector groups,  $n = 6$



and an anti-OPG-neutralization antibody (Figure 3F) when the SSCs were cocultured with monocytes. We found that the in vitro OC formation in the SSC/OC coculture system was significantly rescued, which demonstrates that OASF-induced OPG secretion in SSCs significantly contributed to the osteoclastic suppression (Figure 3E,F) ( $*P < .05$ ).

Increasing evidence has demonstrated that highly expressed ICAM-1 and VCAM-1 contribute to the progression of inflammatory diseases, including osteoarthritis.<sup>36,37</sup> In the current study, we found that incubation with human OASF-induced high expressions of ICAM-1 and VCAM-1 by SSCs (Figure 4A). Functionally, we used blocking antibodies against ICAM-1 and VCAM-1 to directly test whether ICAM-1 and VCAM-1 in SSC mediate OC precursor adhesion. As CD11b<sup>+</sup> cells represent a pivotal subpopulation of OC precursors, we identified a CFSE<sup>+</sup>CD11b<sup>+</sup> cell proportion to evaluate the adhesion capacity of SSCs. As shown in Figure 4B, SSCs captured a smaller proportion of OC precursors in the presence of blocking antibodies than the control. In addition, the blocking effects were antibody dose-dependent (Figure 4C) ( $*P < .05$ ). The results of the SSC/OC coculture experiments further demonstrated their important role in SSC-mediated OC suppression (Figure 4D) ( $*P < .05$ ).

To detect synergistic effects of the adhesion molecules and OPG in SSC-mediated OC suppression in vivo, we infused OPG<sup>knock-down</sup>

SSCs, as well as ICAM-1<sup>high</sup> and VCAM-1<sup>high</sup> SSCs into LPS mice individually. The results of the murine tibia TRAP staining showed that SSC-induced OPG deficiency led to an increased number of OC in situ (Figure 5A,B) ( $*P < .05$ ). In addition, we found that SSC-mediated osteoclast suppression was remarkably enhanced when ICAM-1 or VCAM-1 were genetically overexpressed (Figure 5C,D) ( $*P < .05$ ).

### 3.4 | SSCs suppress inflammatory osteoclastogenesis in a TNF- $\alpha$ dependent manner

To explore how OASF-induced SSC-mediated osteoclast suppression of cytokines, numerous neutralizing antibodies against pro-inflammatory cytokines in human OASF were added to the SSC/OC generation system. We found that the anti-TNF- $\alpha$  antibody greatly blocked the upregulation of OPG (Figure 6A) ( $*P < .05$ ) and cell surface molecules (Figure 6B) ( $*P < .05$ ;  $**P < .01$ ) by SSC, while anti-IFN- $\gamma$ , anti-IL-17A, anti-IL-6, and anti-M-CSF antibodies exerted little effect. In addition, the TNF- $\alpha$  blockage significantly rescued OC formation in the presence of SSCs and OASF (Figure 6C,D) ( $*P < .05$ ). Furthermore, the inflammatory serum from the LPS mouse generated

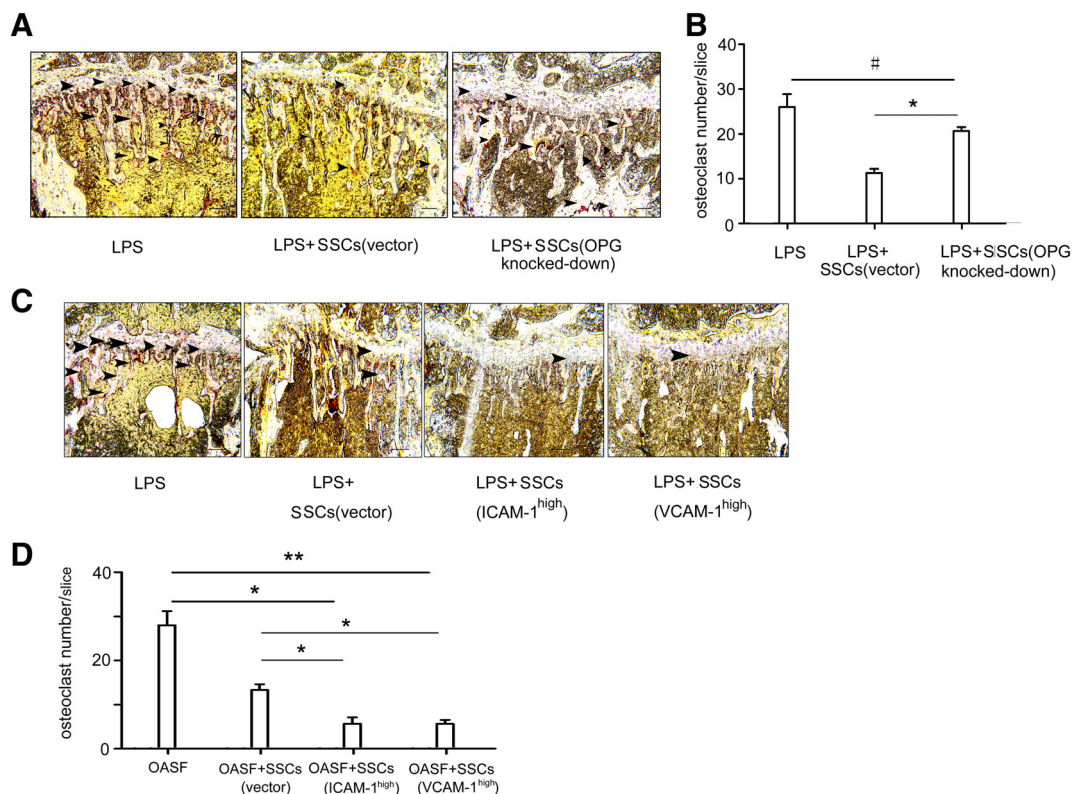


**FIGURE 5** Skeletal stem cells (SSCs) suppress inflammatory osteoclast (OC) formation in vivo through secreted osteoprotegerin (OPG) acting in synergy with ICAM-1 and VCAM-1. A, The OPG stably knocked-down SSCs ( $5 \times 10^5$  SSCs in 100  $\mu$ L PBS per mouse) were intravenously administered to LPS mice. Tartrate-resistant acid phosphatase positive (TRAP<sup>+</sup>) osteoclasts stained in red in murine tibial metaphysis are indicated by arrowheads. B, Comparable to the empty vector group, OPG<sup>low</sup> SSCs exhibited impaired suppressive effects on in situ osteoclast formation.  $P < .05$ ,  $n = 6$ . C, Notably, SSC-mediated osteoclast suppression in vivo was remarkably strengthened when ICAM-1 overexpressing SSCs or VCAM-1 overexpressing SSCs ( $5 \times 10^5$  SSC in 100  $\mu$ L PBS per mouse) were intravenously infused in LPS mice. D, The TRAP stained osteoclasts in red are significantly decreased in vivo.  $*P < .05$ , compared with empty vector groups,  $n = 6$

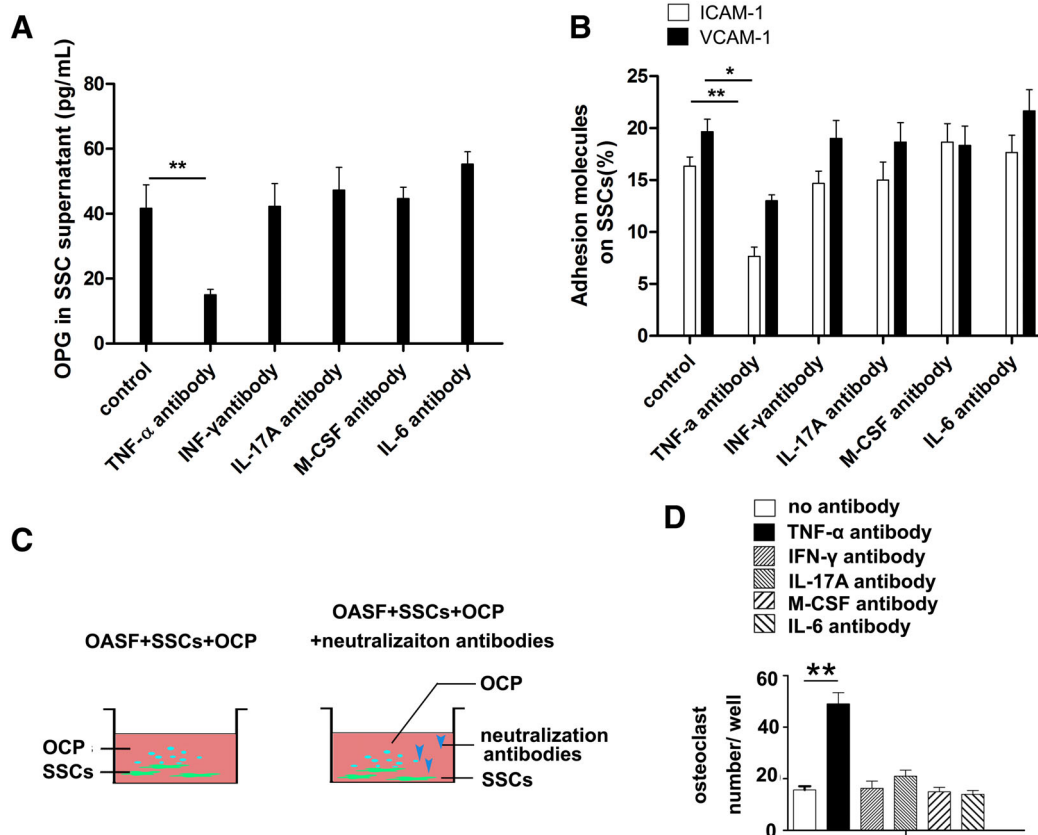


**FIGURE 6** Skeletal stem cells (SSCs) suppress human osteoarthritis synovial fluid (OASF)-induced inflammatory osteoclastogenesis in a TNF- $\alpha$  dependent manner. A, Numerous neutralization antibodies (anti-TNF- $\alpha$ , anti-IFN- $\gamma$ , anti-IL-17A, anti-M-CSF, and anti-IL-6, respectively) were added into SSC/OC culture system (200 ng/mL). The osteoprotegerin (OPG) in the culture medium of each group was detected by ELISA assay. B, The ratios of ICAM-1 or VCAM-1 expressing SSC in each group were determined by flow cytometry. The blockage of TNF- $\alpha$  significantly abolished the OASF-induced upregulation of OPG and cell surface molecules by SSCs. \* $P < .05$ , compared with no antibody group,  $n = 6$ . C, In addition, neutralization antibodies were added into SSC/OC coculture system (200 ng/mL). D, Notably, TNF- $\alpha$  blockage partially reverts the suppressive capacity of SSC on in vitro inflammatory osteoclastogenesis. \* $P < .05$ , compared with no antibody group,  $n = 6$

from the TNF- $\alpha$  knockout (KO) mouse failed to induce SSC-mediated osteoclastic suppression (Figure S1A,B) (\*\* $P < .01$ ).

## 4 | DISCUSSION

In the current study, we found that SSCs inhibit inflammatory osteoclastogenesis via the concerted action of OPG and cell adhesion molecules in vivo and in vitro. Moreover, we demonstrated that TNF- $\alpha$  is indispensable for the suppressive effects.

SSCs are endogenous stem cells in skeletal tissues. Increasing evidence has demonstrated that SSCs are closely involved in bone homeostasis.<sup>1-8,38,39</sup> These cells respond to tissue stress and migrate to sites of injury, supplying new osteoblasts during fracture healing.<sup>40</sup> In addition, SSCs are capable of homing back to the bone marrow after intravenous infusion and providing a supportive environment for hematopoiesis.<sup>41</sup> Notably, our previous studies show that a subpopulation of SSCs remain present in murine bone, and further investigations demonstrated that SSCs play a role as a pivotal regulator in inflammatory responses in vitro and in vivo.<sup>25-27</sup> In the current study, SSCs were harvested from whole long bones of mice to include more SSC populations. Here, we identified a

novel function SSCs in inhibiting inflammatory osteoclastogenesis using an LPS mouse model and human OASF, which deepens the understanding of skeletal biology in bone diseases.

Accumulated studies have demonstrated that ICAM-1 and VCAM-1 are critically involved in various inflammatory pathological diseases, such as osteoarthritis.<sup>36,37</sup> ICAM-1 is highly expressed in OC precursors and stromal cells, including synoviocytes, osteoblasts and periodontal ligament fibroblasts, in osteoarthritis. Although the role of ICAM-1 in osteoclastogenesis has been widely reported, most previous studies have suggested ICAM-1 is a pro-osteoclastic molecule.<sup>36</sup> The expression of ICAM-1 by OC precursors increases during OC formation, and blocking ICAM-1 in OC precursors decreased the number of osteoclasts formed.<sup>42</sup> In addition, ICAM-1-expressing osteoblasts have been proven to support OC formation, and osteoblasts that lack ICAM-1 do not possess this capacity.<sup>36</sup> Further studies show that ICAM-1 is highly expressed in damaged articular and meniscal cartilage in human OA.<sup>36</sup> VCAM-1 is also viewed as an inflammatory mediator in the pathologic process of bone disease. A clinical study concluded that the level of soluble VCAM-1 emerged as a strong and independent predictor of the risk of hip and knee joint replacement due to severe OA.<sup>43</sup> Another study demonstrated VCAM-1 is highly expressed in RA whole-tissue synovial explants.<sup>44</sup> To

the best of our knowledge, few previous studies have demonstrated the protective effects of ICAM-1 and VCAM-1 in bone disease.

Interestingly, Ren et al reported that when mesenchymal stromal cells (MSCs) were cocultured with activated T cells, they significantly upregulated the adhesive capability of T cells.<sup>45</sup> Moreover, the greater the expression of ICAM-1 and VCAM-1 by MSCs is associated with the greater the immunosuppressive effects exhibited by MSCs.<sup>46</sup> Further study showed that T cell-derived inflammatory cytokines induce the expression of ICAM-1 and VCAM-1. Moreover, blocking cell adhesion molecules with neutralization antibodies remarkably decreased the immunosuppressive capacity. These findings demonstrated that inducible ICAM-1 and VCAM-1 were able to recruit more T cells to the proximity of MSCs, which promoted MSC-mediated immunosuppression.<sup>35</sup> Therefore, the work of Ren et al suggested that close proximity is pivotal for MSC-derived factors to modulate T cell proliferation and other immune responses, which indicated a novel function of ICAM-1 and VCAM-1 in immunoregulation by MSCs.<sup>45,46</sup>

In the current study, we were greatly interested in whether these molecules were involved in SSC-mediated osteoclastic suppression. We found that ICAM-1 and VCAM-1 play pivotal roles in osteoclastic regulation by SSCs in a similar manner to that of immunoregulation by MSCs. Induced by TNF- $\alpha$  in OASF, the SSCs highly expressed ICAM-1 and VCAM-1. An adhesion assay indicated that the upregulated adhesion molecules captured more CD11b<sup>+</sup> OC precursors. Most importantly, TNF- $\alpha$  promoted-SSCs secreted more OPG. As previously established, OPG is a decoy receptor for RANKL and has been identified as a key suppressor of osteoclastogenesis. Therefore, we suggest that SSCs capture more OC precursors and enable OPG to work in proximity. To validate this idea, the expression of OPG by SSCs was inhibited by both RNAi and OPG-neutralization antibody. The suppressive effect of osteoclastogenesis was remarkably decreased when OPG was blocked. The data strongly support the hypothesis that SSCs inhibit inflammatory OC formation in a "capture and educate" manner. Moreover, SSC administration did not significantly affect osteoclast formation in PBS mice, which suggested that SSCs may modulate inflammatory osteoclastic activity in a way that is different from that in noninflammatory microenvironments.

Our findings have important implications for the treatments of bone disease. Although many types of stem cells have been used to treat bone diseases in previous decades, the emergence of SSCs brings a new choice for therapy. The antiosteoclastic capacity of SSCs may be useful in the treatment of inflammatory joint diseases. On the other hand, in addition to the therapeutic effects of exogenous SSCs in skeletal repair, endogenous SSCs may be a novel cell target to reduce osteoclastic resorption in bone disease.<sup>45,46</sup>

Nevertheless, we must acknowledge several limitations in our study. First, a bone resorption assay is important to evaluate osteoclastogenesis.<sup>9,47</sup> Determining the roughness of the dentin slices by profilometry in further investigations may be helpful to measure the resorption pit.<sup>48</sup> Second, the molecular mechanisms that control the expression of ICAM-1 and VCAM-1, as well as OPG expression by SSCs should be clarified in future investigations. Third, additional explorations are needed to determine whether other factors contribute to SSC-mediated suppression of inflammatory osteoclastogenesis in vitro and in vivo, and high-throughput assays may be helpful to address this issue.

Fourth, the number of human OASF samples used in the current study is relatively small, and the clinical sample size should be enlarged to reinforce the findings in further studies.

## 5 | SUMMARY

In the present study, we reported a new role for SSCs in the suppression of inflammatory osteoclastogenesis. In addition, our study shows synergistic mechanisms that limit bone erosion during joint inflammation by SSCs. Importantly, a comprehensive analysis of SSCs in human bone diseases is needed to further investigate and clarify these results.

## ACKNOWLEDGMENTS

This study was supported by the National Natural Science Foundation of China (81572159, 81871771, 81500083, 81371945, 81101342) and the Beijing Natural Sciences Grants (7182123, 7192203).

## CONFLICT OF INTEREST

The authors indicated no potential conflicts of interest.

## AUTHOR CONTRIBUTIONS

X.L.: collection and/or assembly of data, data analysis and interpretation, manuscript writing; L.D.: collection and/or assembly of data, data analysis and interpretation, manuscript writing, financial support; Y.-X.W.: collection and/or assembly of data, data analysis and interpretation, manuscript writing, provision of study material or patients; Z.-L.L.: provision of study material or patients; Q.W., Z.-D.Z.: collection and/or assembly of data, data analysis and interpretation; S.Z.: collection and/or assembly of data; H.W., C.-T.W.: administrative support; N.M.: financial support, conception and design, final approval of manuscript; H.Z.: manuscript writing, financial support, conception and design, final approval of manuscript.

## DATA AVAILABILITY STATEMENT

The data that support the findings of this study are available from the corresponding author upon reasonable request.

## ORCID

Heng Zhu  <https://orcid.org/0000-0002-8408-3821>

## REFERENCES

1. Bianco P, Robey PG. Skeletal stem cells. *Development*. 2015;142:1023-1027.
2. Chan CK, Seo EY, Chen JY, et al. Identification and specification of the mouse skeletal stem cell. *Cell*. 2015;160:285-298.
3. Worthley DL, Churchill M, Compton JT, et al. Gremlin 1 identifies a skeletal stem cell with bone, cartilage, and reticular stromal potential. *Cell*. 2015;160:269-284.
4. Tang Y, Feinberg T, Keller ET, et al. Snail/Slug binding interactions with YAP/TAZ control skeletal stem cell self-renewal and differentiation. *Nat Cell Biol*. 2016;18:917-929.
5. Maruyama T, Jeong J, Sheu TJ, et al. Stem cells of the suture mesenchyme in craniofacial bone development, repair and regeneration. *Nat Commun*. 2016;7:10526.
6. Shi Y, He G, Lee WC, et al. Gli 1 identifies osteogenic progenitors for bone formation and fracture repair. *Nat Commun*. 2017;8:2043.



7. Debnath S, Yallowitz AR, McCormick J, et al. Discovery of a periosteal stem cell mediating intramembranous bone formation. *Nature*. 2018; 562:133-139.
8. Chan CKF, Gulati GS, Sinha R, et al. Identification of the human skeletal stem cell. *Cell*. 2018;175:43-56.e21.
9. Teitelbaum SL. Bone resorption by osteoclasts. *Science*. 2000;289: 1504-1508.
10. Boyle WJ, Simonet WS, Lacey DL. Osteoclast differentiation and activation. *Nature*. 2003;423:3342-3373.
11. Arnett TR, Orriss IR. Metabolic properties of the osteoclast. *Bone*. 2018;115:25-30.
12. Saberi Hosnijeh F, Bierma-Zeinstra SM, Bay-Jensen AC. Osteoarthritis year in review 2018: biomarkers (biochemical markers). *Osteoarthritis Cartilage*. 2019;27:412-423.
13. McGonagle D, Baboolal TG, Jones E. Native joint-resident mesenchymal stem cells for cartilage repair in osteoarthritis. *Nat Rev Rheumatol*. 2017;13:719-730.
14. Nefla M, Holzinger D, Berenbaum F, et al. The danger from within: alarmins in arthritis. *Nat Rev Rheumatol*. 2016;12:669-683.
15. Badawy T, Kyumoto-Nakamura Y, Uehara N, et al. Osteoblast lineage-specific cell-surface antigen (A7) regulates osteoclast recruitment and calcification during bone remodeling. *Lab Invest*. 2019;99:866-884.
16. Batra N, Kar R, Jiang JX. Gap junctions and hemichannels in signal transmission, function and development of bone. *Biochim Biophys Acta*. 1818;2012:1909-1918.
17. Cheung WY, Simmons CA, You L. Osteocyte apoptosis regulates osteoclast precursor adhesion via osteocytic IL-6 secretion and endothelial ICAM-1 expression. *Bone*. 2012;50:104-110.
18. Lu X, Mu E, Wei Y, et al. VCAM-1 promotes osteolytic expansion of indolent bone micrometastasis of breast cancer by engaging  $\alpha 4 \beta 1$ -positive osteoclast progenitors. *Cancer Cell*. 2011;20:701-714.
19. Takayanagi H, Ogasawara K, Hida S, et al. T-cell-mediated regulation of osteoclastogenesis by signalling cross-talk between RANKL and IFN- $\gamma$ . *Nature*. 2000;408:600-605.
20. Takayanagi H. New developments in osteoimmunology. *Nat Rev Rheumatol*. 2012;8:684-689.
21. Ren X, Zhou Q, Foulad D, et al. Osteoprotegerin reduces osteoclast resorption activity without affecting osteogenesis on nanoparticulate mineralized collagen scaffolds. *Sci Adv*. 2019;5:eaaw4991.
22. Guo Z, Li H, Li X, et al. In vitro characteristics and in vivo immunosuppressive activity of compact bone-derived murine mesenchymal progenitor cells. *STEM CELLS*. 2006;24:992-1000.
23. Zhu H, Guo ZK, Jiang XX, et al. A protocol for isolation and culture of mesenchymal stem cells from mouse compact bone. *Nat Protoc*. 2010;5:550-560.
24. Wang K, Li J, Li Z, et al. Chondrogenic progenitor cells exhibit superiority over mesenchymal stem cells and chondrocytes in platelet-rich plasma scaffold-based cartilage regeneration. *Am J Sports Med*. 2019; 47:2200-2215.
25. Li H, Guo ZK, Li XS, et al. Functional and phenotypic alteration of intrasplenic lymphocytes affected by mesenchymal stem cells in a murine allosplenocyte transfusion model. *Cell Transplant*. 2007;16:85-95.
26. Li H, Guo Z, Jiang X, et al. Mesenchymal stem cells alter migratory property of T and dendritic cells to delay the development of murine lethal acute graft-versus-host disease. *STEM CELLS*. 2008;26:2531-2541.
27. Zhu H, Yang F, Tang B, et al. Mesenchymal stem cells attenuated PLGA-induced inflammatory responses by inhibiting host DC maturation and function. *Biomaterials*. 2015;53:688-698.
28. Aletaha D, Neogi T, Silman AJ, et al. 2010 Rheumatoid arthritis classification criteria: an American College of Rheumatology/European League Against Rheumatism collaborative initiative. *Arthritis Rheum*. 2010;62:2569-2581.
29. Peterfy CG, Guermazi A, Zaim S, et al. Whole-Organ Magnetic Resonance Imaging Score (WORMS) of the knee in osteoarthritis. *Osteoarthritis Cartilage*. 2004;12:177-190.
30. Xu FF, Zhu H, Li XM, et al. Intercellular adhesion molecule-1 inhibits osteogenic differentiation of mesenchymal stem cells and impairs bio-scaffold-mediated bone regeneration in vivo. *Tissue Eng Part A*. 2014;20:2768-2782.
31. Chen H, Zhu H, Chu YN, et al. Construction of mouse VCAM-1 expression vector and establishment of stably transfected MSC line C3H10T1/2. *J Exp Hematol*. 2014;22(5):1396-1401.
32. Abu-Amer Y, Ross FP, Edwards J, Teitelbaum SL. Lipopolysaccharide-stimulated osteoclastogenesis is mediated by tumor necrosis factor via its P55 receptor. *J Clin Invest*. 1997;100(6):1557-1565.
33. Kollet O, Dar A, Shivtiel S, et al. Osteoclast degrade endosteal components and promote mobilization of hematopoietic progenitor cells. *Nat Med*. 2006;12(6):657-664.
34. Kwak HB, Lee BK, Oh J, et al. Inhibition of osteoclast differentiation and bone resorption by rotenone, through down-regulation of RANKL-induced c-Fos and NFATc1 expression. *Bone*. 2010;46(3):724-731.
35. Ren G, Zhao X, Zhang L, et al. Inflammatory cytokine-induced intercellular adhesion molecule-1 and vascular cell adhesion molecule-1 in mesenchymal stem cells are critical for immunosuppression. *J Immunol*. 2010;184:2321-2328.
36. Lavigne P, Benderdour M, Lajeunesse D, et al. Expression of ICAM-1 by osteoblasts in healthy individuals and in patients suffering from osteoarthritis and osteoporosis. *Bone*. 2004;35:463-470.
37. Schett G, Kiechl S, Bonora E, et al. Vascular cell adhesion molecule 1 as a predictor of severe osteoarthritis of the hip and knee joints. *Arthritis Rheum*. 2009;60:2381-2389.
38. Mizuhashi K, Ono W, Matsushita Y, et al. Resting zone of the growth plate houses a unique class of skeletal stem cells. *Nature*. 2018;563:254-258.
39. Kuwahara ST, Serowoky MA, Vakhshori V, et al. Sox9+ messenger cells orchestrate large-scale skeletal regeneration in the mammalian rib. *Elife*. 2019;8:e40715.
40. Park D, Spencer JA, Koh BI, et al. Endogenous bone marrow MSCs are dynamic, fate-restricted participants in bone maintenance and regeneration. *Cell Stem Cell*. 2012;10:259-272.
41. Hu X, Garcia M, Weng L, et al. Identification of a common mesenchymal stromal progenitor for the adult haematopoietic niche. *Nat Commun*. 2016;7:13095.
42. Bloemen V, de Vries TJ, Schoenmaker T, et al. Intercellular adhesion molecule-1 clusters during osteoclastogenesis. *Biochem Biophys Res Commun*. 2009;385:640-645.
43. Chou CH, Attarian DE, Wisniewski HG, et al. TSG-6 - a double-edged sword for osteoarthritis (OA). *Osteoarthritis Cartilage*. 2018;26:245-254.
44. McGarry T, Orr C, Wade S, et al. JAK/STAT blockade alters synovial bioenergetics, mitochondrial function, and proinflammatory mediators in rheumatoid arthritis. *Arthritis Rheumatol*. 2018;70:1959-1970.
45. Ren G, Zhang L, Zhao X, et al. Mesenchymal stem cell-mediated immunosuppression occurs via concerted action of chemokines and nitric oxide. *Cell Stem Cell*. 2008;2:141-150.
46. Ren G, Roberts AI, Shi Y. Adhesion molecules: key players in Mesenchymal stem cell-mediated immunosuppression. *Cell Adh Migr*. 2011;5:20-22.
47. Boyle WJ, Simonet WS, Lacey DL. Osteoclast differentiation and activation. *Nature*. 2003;423(6937):337-342.
48. Rumpel M, Würger T, Roschger P, et al. Osteoclasts on bone and dentin in vitro: mechanism of trail formation and comparison of resorption behavior. *Calcif Tissue Int*. 2013;93(6):526-539.

## SUPPORTING INFORMATION

Additional supporting information may be found online in the Supporting Information section.

**How to cite this article:** Li X, Ding L, Wang Y-X, et al. Skeletal stem cell-mediated suppression on inflammatory osteoclastogenesis occurs via concerted action of cell adhesion molecules and osteoprotegerin. *STEM CELLS Transl Med*. 2020;9: 261-272. <https://doi.org/10.1002/sctm.19-0300>